24th COBEM - 2017

24th ABCM International Congress of Mechanical Engineering
December 3-8, 2017, Curitiba, PR, Brazil

COBEM-2017-1968
SIMPLIFIELD THERMAL ANALYSIS AND OPTMIZATION OF A BETA TYPE STIRLING CYCLE

Handerson Corrêa Gomes[1]
Michel Fábio de Souza Moreira[2]
Lucas Paglioni Pataro Faria[3]
Christopher Soares de Figueiredo[4]
Filipe Ferreira Dias Fonseca[5]
Caíque Augusto Teixeira[6]
David Henrique Do Nascimento Viola[7]
Centro Universitário Newton Paiva, Department of Mechanical Engineering, Street José Cláudio Rezende, number 420 – District Estoril - Belo Horizonte - MG – Zip Code 30.494-230 – Brazil
E-mails: [1]handerson.correa@gmail.com, [2]michelsatriani@gmail.com, [3]lucas.faria@newtonpaiva.com, [4]christopher.figueiredo@gmail.com, [5]filipeengmec@gmail.com, [6]caiquemecanica@outlook.com, [7]dhviola@gmail.com.

Abstract. *In this work, it is performed the thermal analysis and optimization of a beta type Stirling cycle. The analysis was based on Thermodynamics. The optimization was performed using a Genetic algorithm with mono objective function. The cycle behavior operating with air, hydrogen and helium, and in different temperatures, to investigate which was more appropriate to obtain better power and efficiency. The Hydrogen showed better properties, but it presents a dangerous disadvantage, its high flammability. That is the reason why helium is gaining space to replace hydrogen. This fluid presents similar characteristics and properties with the hydrogen though it is not flammable. The air was also tested in computational engine simulation. The air is abundant and inexpensive, but presented a low thermal efficiency to the cycle. The results obtained in the analytic computational simulation and the experimental results have presented the deviation into the order of 17,4% for the same turn round conditions considering air as work fluid. With the optimization it can be observed that under specific conditions (hardly reached in experiment) the cycle can reach high yeld mainly with the reduction of the temperature differnces between the sources.*

Keywords: *Thermal analysis, optimization, Stirling cycle, Stirling engine, efficiency.*

1. INTRODUCTION

The Stirling engine is considered an external combustion type, generating work from any sort of heat source, like gases, wood, biomass and even solar energy. Duffie et al. (1991) reported that the Stirling is the most efficient thermodynamic cycle available for work performance. The Beta type Stirling engine, activated by solar energy makes it possible to use this source of energy as fuel (Garg, 1987). For the correct start of a Stirling engine, it is necessary to study it though thermal analysis and use optimization techniques. Such studies can demonstrate better efficiency for various operational parameters and different fluids. Several computational and experimental studies on the Stirling engine have been carried out

Kongtragool and Wongwises (2006) carried out in their article a theoretical investigation on the thermodynamic analysis of a Stirling engine. An isothermal model is developed by an imperfect regeneration Stirling engine with dead volumes of hot space, cold space and regenerator and its effective temperature is an arithmetic mean of the heater and cooler temperature. Numerical simulation is performed and the effects of the regenerator effectiveness and dead volumes are studied. Results from this study indicate that the engine interaction is affected by only the dead volumes, while the heat input and engine efficiency are affected by both the regenerator effectiveness and dead volumes.

The engine interaction decreases with increasing dead volume. The heat input increases with increasing dead volume and decreasing regenerator effectiveness.

Kongtragool and Wongwises (2006) showed in their study that the engine efficiency decreases with increasing dead volume and decreasing regenerator effectiveness. Parlak et.al. (2009) performed a thermodynamic analysis of a gamma type Stirling engine is performed by using a quasi-steady flow model based on Urieli and Berchowitz's works. A FORTRAN code is developed to solve the derived equations of the mass and the energy for all process parameters like pressure, temperature, mass flow, dissipation and convection losses for the different spaces (compression space, cooler,

regenerator, heater and expansion space) as a function of the crank angle. According Parlak et.al. (2009) the developed model gave more precise results for the pressure profile than the models available in the literature. Tlili, Timoumi and Nasrallah (2008) presents a technical innovation, study of solar power system based on the Stirling dish (SD) technology and design applicable considerations must be observed during the design development for a Stirling engine provided with a differential temperature average for solar application. The power source will be solar dish/Stirling with average concentration ratio, which will supply a temperature constant source of 320°C. Hence, the system design is based on a temperature difference of 300°C, assuming that the sink is kept at 20°C.

During the preliminary design stage, the critical parameters of the engine design are determined according to the dynamic model with losses energy and pressure drop in heat exchangers was used during the design optimization stage in order to establish a complete analytical model for the engine. The heat exchangers are designed to be of high effectiveness and low pressure-drop. Erbay and Yavuz (1997) performed an Analysis of the Stirling heat engine at maximum power conditions. According to the authors The Stirling heat engine operating in a closed regenerative thermodynamic cycle is analyzed. In this study Polytropic processes are used for the power and displacement pistons. Following regeneration, the maximum power density and efficiency are found and the compression ratio at maximum power density is determined. Ahmadi et. Al. (2013) performed a study of a solar-powered high temperature differential Stirling engine was considered for optimization using multiple criteria. A thermal model was developed so that the output power and thermal efficiency of the solar Stirling system with finite rate of heat transfer, regenerative heat loss, conductive thermal bridging loss, finite regeneration process time and imperfect performance of the dish collector could be obtained.

The output power and overall thermal efficiency were considered for simultaneous maximization. Multi-objective evolutionary algorithms (MOEAs) based on the NSGA-II algorithm was employed while the solar absorber temperature and the highest and the lowest temperatures of the working fluid were considered the decision variables. The Pareto optimal frontier was obtained and a final optimal solution was also selected using various decision-making methods including the fuzzy Bellman–Zadeh, LINMAP and TOPSIS. It was found that multi-objective optimization could produce results with a relatively low deviation from the ideal solution in comparison to the conventional single objective approach. Furthermore, it was shown that, if the weight of thermal efficiency as one of the objective functions is considered to be greater than weight of the power objective, a lower absorber temperature and a low temperature ratio should be considered in the design of the Stirling engine. Mohammad (2015) employed a new generation of intelligent models named “least square support vector machine (LSSVM)” to predict output power and shaft torque of Stirling engines.

To build, train and test the LSSVM model, various accurate experimental data from open literature are employed. The outputs of the LSSVM model are compared to experimental ones and statistical parameters of the LSSVM model including correlation coefficient, average absolute relative deviation (AARD) and root mean square error (RMSE) are calculated. According to the results obtained via LSSVM model, the LSSVM model can predict output power and shaft torque of Stirling heat engine with reasonable and acceptable accuracy. Finally, the LSSVM model can help us in designing of Stirling engine with low degree of uncertainty and high precision.

In this paper there is an objective performed a numerical and experimental analysis of a beta alpha type Stirling engine. The numerical analysis is performed through the implementation of a thermodynamic model as described below. Then the Genetic Algorithm (Holland, 1975) was used to optimize, in a first simulation, the efficiency of the motor that was maximized as a mono objective function. In the second simulation, the heat absorbed in the cycle was maximized. Experiments were performed with a commercial alpha type Stirling engine using air and helium as working fluid.

2. COMPUTATIONAL PROCEDURE

The Stirling cycle comprises four processes: constant temperature compression; constant volume heating; expansion at constant temperature; and heat rejection at constant volume.

Nomenclature

Q_H = Heat absorbed [kJ]	η = Cycle efficiency
W_{BC} = Expansion work [kJ]	R = Gas constant [kJ/kg-K]
W_{DA} = Compression work [kJ]	V_A = Compressed volume hot chamber without heat absorption [m³]
W = Total work [kJ]	V_B = Compressed volume hot chamber with heat absorption [m³]
T_1 = High temperature [K]	V_C = Expanded Volume cold chamber without heat rejection [m³]
T_2 = Low temperature [K]	
ΔT = Temperature variation ($T_1 - T_2$) [K]	V_D = Expanded Volume cold chamber with heat rejection [m³]
T_c = Compression Ratio (V_C / V_B)	

On Fig. 1, a Stirling cycle is presented in a Thermodynamic diagram P – V.

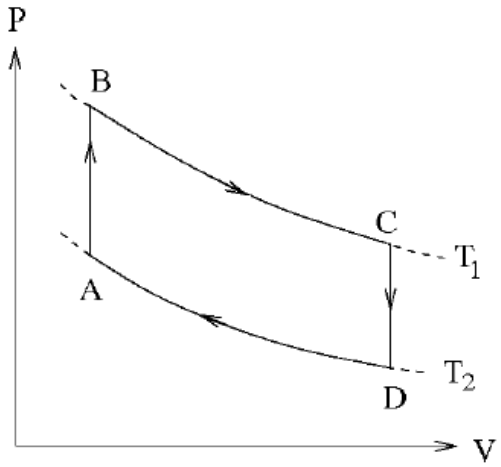

Figure 1 – Graphic P-V Stirling cycle.
Source: (DUARTE, TOLEDO E OLIVEIRA, 2014)

Based on Fig. 1, the heat is absorbed in the beginning of the cycle, part BC, and can be obtained through the equation 1.

$$Q_H = Q_{BC} = W_{BC} = RT_1 \ln(V_C / V_B) \quad \text{(Eq. 1)}$$

As there is no variation of volume in the processes CD e AB (isochorics, Fig. 1), there's no work performance, so, by equation 2.

$$W_{CD} = W_{BC} = 0 \quad \text{(Eq. 2)}$$

The overall work is the sum of the expansion and compression works (Equations 3 and 4), because the energy spend on compression is part of the absorbed heat.

$$W = W_{BC} + W_{DA} \quad \text{(Eq. 3)}$$

$$W = RT_1 \ln(V_C / V_B) + RT_2 \ln(V_A / V_D) \quad \text{(Eq. 4)}$$

Efficiency is the satisfactory result of the work performed, being the quotient of the energy spend to perform the work intended and the consumed energy (Equations 5 - 6).

$$\eta = \frac{W}{Q_H} = \frac{RT_1 \ln(V_C / V_B) + RT_2 \ln(V_A / V_D)}{RT_1 \ln(V_C / V_B)} \quad \text{(Eq. 5)}$$

$$\eta = 1 + \frac{T_2 \ln(V_A / V_D)}{T_1 \ln(V_C / V_B)} \quad \text{(Eq. 6)}$$

As, $V_C = V_D$ e $V_A = V_B$, we have the equation 7.

$$\eta = 1 + \frac{T_2 \ln(V_B / V_C)}{T_1 \ln(V_C / V_B)} \quad \text{(Eq. 7)}$$

Therefore, the efficiency is obtained through equation 8.

$$\eta = 1 - \frac{T_2}{T_1} \quad \text{(Eq. 8)}$$

On equation 8 the calculated efficiency equals a Carnot cycle engine efficiency, where T_1 is the high temperature and T_2 is the low temperature. This way, a Stirling cycle presents a high efficiency, equivalent a Carnot cycle engine.

3. EXPERIMENTAL PROCEDURE

In order to perform with the experimental tests with air and Helium as working fluid, adjustments were made to the conventional heat exchange system in the commercial Stirling engine (Fig. 2). The original tube provide with the commercial Stirling engine responsible for transporting the fluid between the chambers was replaced by a pneumatic polyurethane crosshead, two pins for manual locking and polyurethane tubes all with 10Bar working capacity and maximum temperature of 60°C as shown in Fig 3. This modification gave the experiment the replacement of the working fluid within the chambers.

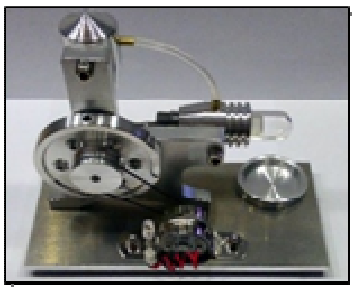

Figure 2 – Commercial Stirling engine.

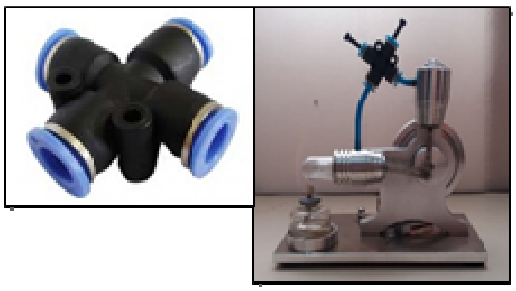

Figure 3 – Modified Stirling engine.

After the implementation of the mathematical model presented in this study, the efficiency and cycle work were calculated for experimentally obtained temperatures. These temperatures were obtained from measurements made on the external surface of the cold chamber (cylinder-piston return assembly) and on the surface of the hot-chamber (cylinder-piston power assembly). A Minipa MDT-2244B tachometer was used for rotation measurements (Fig. 4-A). A DT830B multimeter was used for measuring the electrical current and voltage (Fig. 4-B). A Fluke model 62 MINI laser - focused pyrometer was used for temperatures measurements (Fig. 4-C).

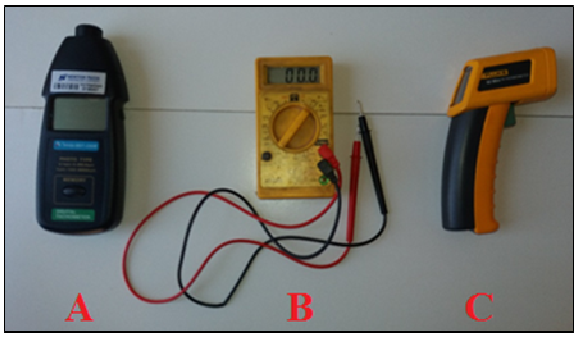

Figure 4 – Measuring instruments used in the research: (a) Minipa brand tachometer MDT-2244B, (b) DT830B commercial multimeter (c) Fluke model 62 MINI with laser focus.

The experimental results were obtained for Air and Helium. The first of these fluids have the gas constant equal to R_{Air} = 0.277kJ/(kg.K), and the second has R_{Helium} = 2.0771 kJ/(kgK) (Sonntag and Borgnakke, 2006). In order to obtain the experimental results in a closed place, alcohol 96 (ethyl alcohol 98.2º INPM) was used to drive the motor. When the motor entered the relative steady state, its measurements were carried out. In addition to the temperature and the rotational measurements, electrical current and voltage were also measured with a multimeter. The measurements of these quantities were carried out from a generator associated to the base of the electric motor (DC motor) associated with the studied Stirling motor. The engine was initially driven with atmospheric air and then with Helium. To perform with the work fluid exchange, Helium initially stored in the cylinder was collected and stored in latex balloons and subsequently injected into the engine chambers with the aid of a pneumatic hose connected to one of the outlets of the crosshead already coupled to the Stirling engine system.

4. RESULTS AND DISCUSSION

4.1. Analytical results without optimization

The simplified Stirling engine analysis was performed implementing the previously presented equations on MATLAB® software. The cycle operating in higher temperatures generates higher works, although is subject to losses (Fig. 5). And if the quotient between the low temperature (T2) and the high temperature (T1) do not increase in the same or higher proportion that the proportion of work temperature increase, although higher work values, the efficiency is reduced. However, higher work values are necessary to provide engines with higher power and torque for the compression ratio being Tc = 10.

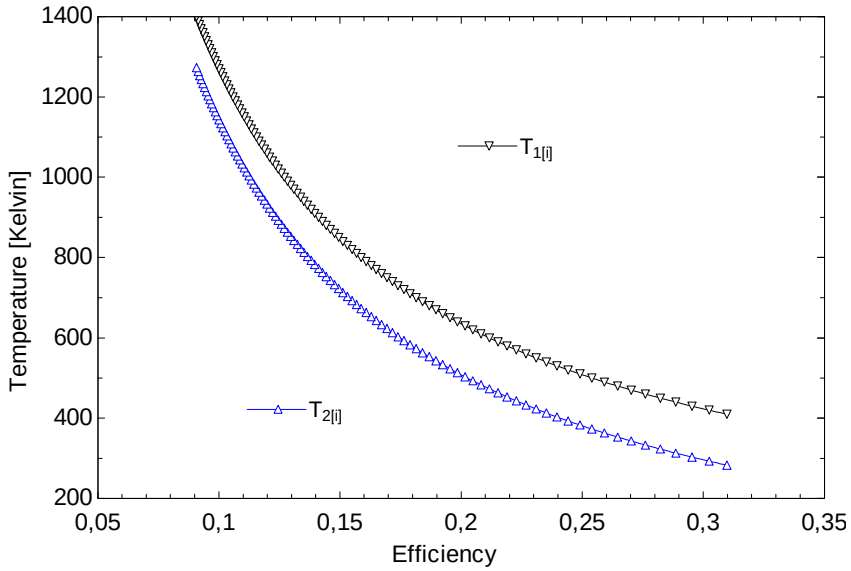

Figure 5 – Graphic showing cycle efficiency according to high and low temperature variation.

Figure 5 illustrates the loss, although the work temperature is increasing, this occurs due the proportion of low and high temperatures increment are different. Figure 6 shows the efficiency decrease with increase of the absorbed heat. The more heat absorption, more work is generated, which is necessary for powerful engines with high torque, yet, there will be more losses what will reduce the efficiency.

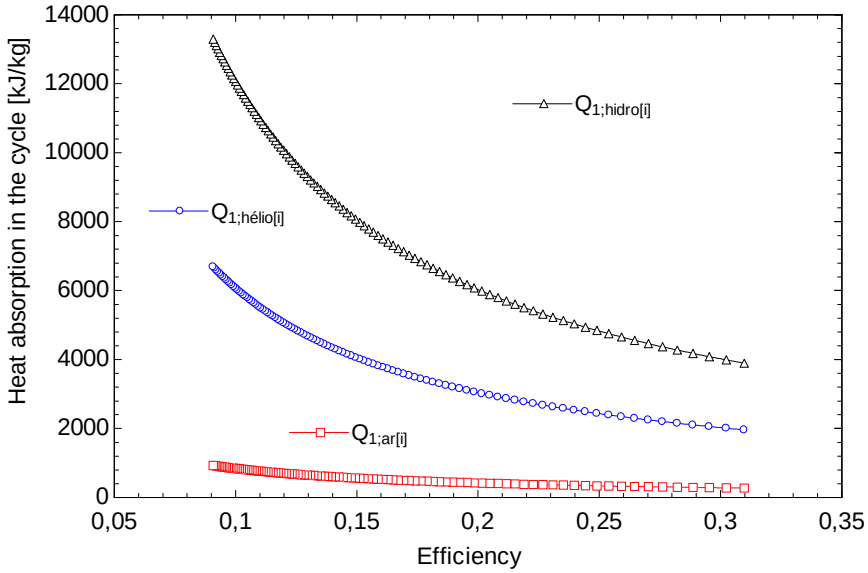

Figure 6 – Graphic showing efficiency according to heat absorption in the cycle.

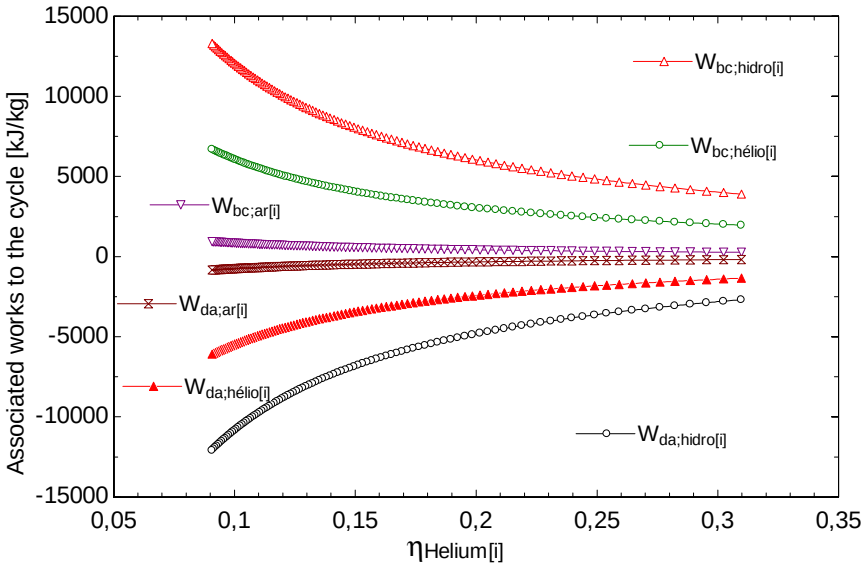

Figure 7 – Graphic showing cycle efficiency according to associated works to the cycle.

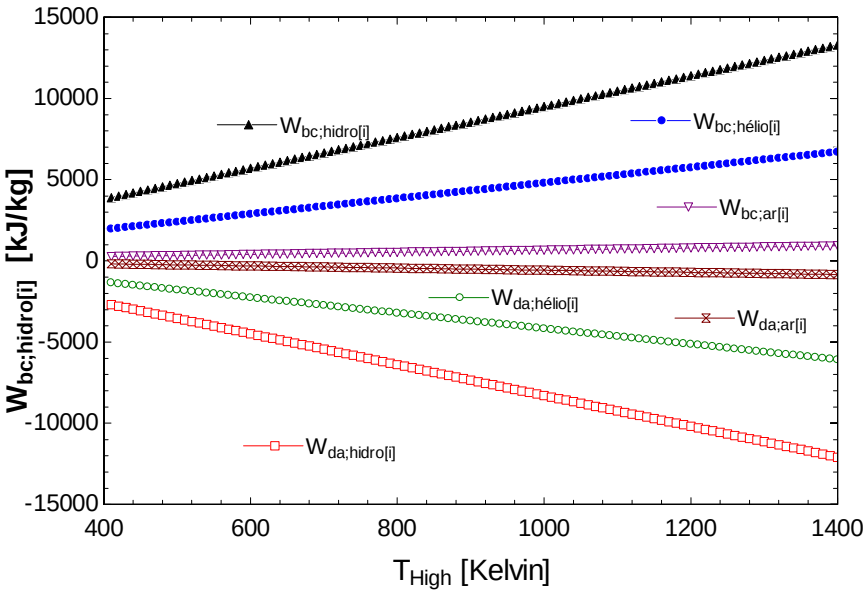

Figure 8 – Graphic showing works involved in the cycle according to high temperature increment.

Figures 7 and 8 illustrates the behaviour of the expansion and compression works. In Fig. 7 is noticeable the approach of the works as the efficiency increases, due the high and low temperature bands choice. Higher works, although, with lower efficiency, because the low and high temperatures are closer as seen on Fig. 6. Now on Fig. 8, the increase of the expansion and compression works proportionally to the high temperature increase. But, however the expansion and compression work increase, the total work will only be greater if the quotient between the high and low temperatures is high.

4.2. Results with mono objective optimization for air as working fluid

The thermodynamic model has presented that the efficiency was maximized based on the Genetic algorithm, considering operating intervals of the alpha type Stirling motor presented in the literature. The results of the simulation are presented as a function of the variables temperature. The Genetic algorithm was used due to its simplicity, robustness and to be presented in the MATLAB® software routine. Despite being a stochastic algorithm it has often been used in direct search methodologies because of its non-fixation around local minimums and maximums as it occurs in deterministic direct search methods. The Fig. 9 illustrates the behavior of the efficiency with the temperatures from Genetic Algorithm. In this figure it is observed that the higher the variation of the temperatures the lower the efficiency. This is due to the greater amount of energy in use by the Stirling cycle which provides greater thermal losses. However, equal efficiency (~ 0.54) is observed for the three curves shown in Fig. 9. The upper curve must be considered due to the greater amount of work generated by the cycle.

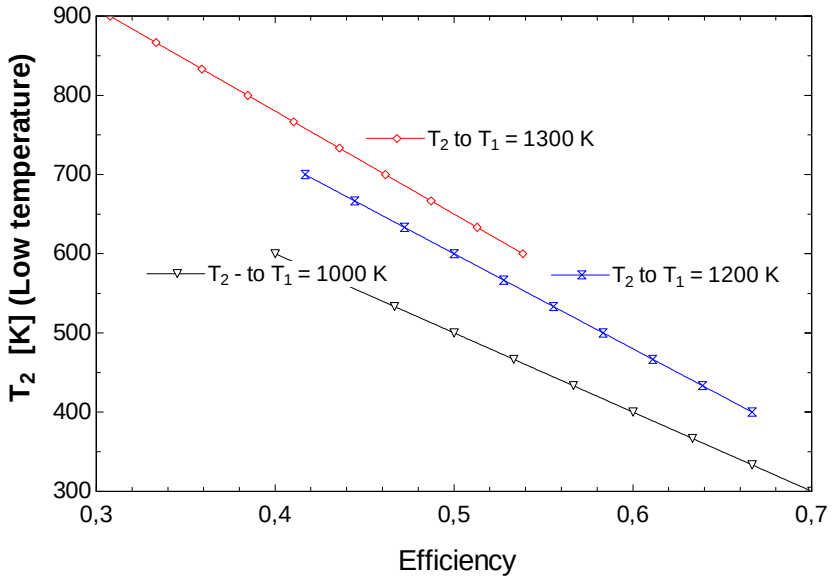

Figure 9 – Graphic showing efficiency in function of the working temperatures from the genetic algorithm

4.3. Experimental results and simulation analytic

The experimental results obtained are presented in Tab. 1.

Table 1 – Measurements performed indoor using ethyl alcohol 92.8º INPM as fuel and air as working fluid.

Rotation in rpm (±5,5%)	High temperature in °C (±3,5%)
1780	-
1850	230
1950	223
1980	220
1850	257

The results presented on Tab. 1 were obtained through an indoor test using ethyl alcohol 92,8% INPM as fuel and air as working fluid. The experiment results were of hard obtainment due to the used measuring instruments which do not have automatic and programmable synchronism and that perform with the accurate measures. Other factor of difficult prediction refers to the combustion process, which is stochastic, difficult to control and influences all other parameters to be measured. After evidenced the performed measuring difficult, other measuring were performed concerning more with the time interval between the measuring than the accurate values, due to high parameters variation rates to be measured, probably influenced by the alcohol combustion process.

Thus, in the second battery of tests it was observed that with air, as working fluid, the rotations were between 1800 and 2000 rpm and the temperature of the hot chamber (cylinder piston power assembly) varied for that rotation range of 180°C at 200°C. In a third battery of tests, still using air, the rotational variation was observed between 1900 and 2000 rpm and with a hot chamber temperature of approximately 230°C. The temperature of the hot chamber was evaluated on the glass surface (cylinder power piston). The temperatures measured on the aluminum surface of the cold chamber presented a temperature average of 33ºC. The temperatures measured on the aluminum surface near the hot chamber presented a temperature average of 40ºC.

For the experiments performed with helium as working fluid (fourth battery of tests) it was observed that the rotation was ranging from 2200rpm to 2454rpm and a temperature average in the hot chamber of 230ºC. The temperatures measured on the aluminum surface of the cold chamber have presented a temperature average of 36ºC. The temperatures measured on the aluminum surface near the hot chamber have presented a temperature average of 40ºC. In the fifth battery of tests, using helium as working fluid, it was observed that the rotation was ranging from 2300rpm to 2602rpm. The temperatures measured on the aluminum surface of the cold chamber have ranged from 33°C to 36°C. The temperatures measured on the aluminum surface near the hot chamber have presented a temperature average from 45°C to 50°C. After the fifth battery of tests, voltage and current measurements were performed between

rotations ranging from 2300 to 2602rpm. In these measurements, the voltage did not change the value of the rotation, but when measuring the electric current the rotation fell drastically: (a) 500rpm; 0.6A; 5.6V; helium as working fluid (mean values) and (b) 480rpm; 0.4A; 4.5V; transition from helium to the working fluid (mean values). This transition between the work fluids was analyzed by the reduction of the motor rotation with the time, due to the helium leakage and natural replacement with the air. The power provided by the motor, calculated by these last measurements was respectively 3.36 watts with efficiency of about 0.2 and 1.8 watts with efficiency of 0.15.

For the computational simulation, the measured data served as turn round conditions for the model. In addition, it was necessary to calculate the volumes in the PMS (Upper Dead Point) and the PMI (Lower Dead Point). The calculated volume in PMS was 1.10521.10-6 m3 and in the PMI was 2.19695.10-6 m3. For these values, the engine studied has presented a compression rate of 1,988, much lower than to those found in engines based on the Otto cycle. For the first battery of tests, with turn round conditions presented in Tab. 1 and simulations with air, from the implemented model the results shown in Fig. 10 are shown below.

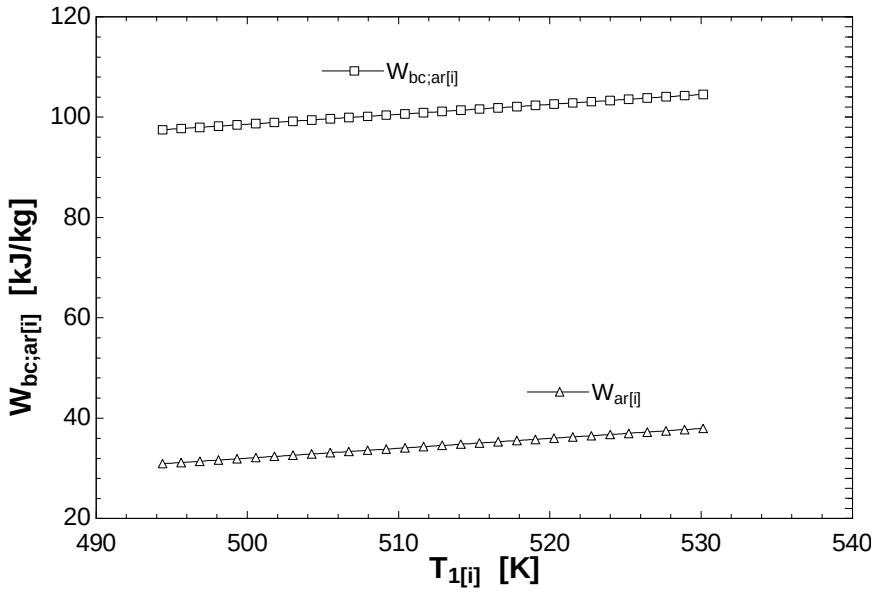

Figure 10 – Graphic showing the specific work produced in the expansion $Wbc_{air}[i]$, and specific work made available by the engine, $W_{air}[i]$, after use this work in the cold chamber (cylinder-piston return assembly) for the engine working with air.

In Fig. 10, it is observed that for a constant temperature of the cold chamber only the specific expansion work, Wbc_{air}, increases with the increase of the temperature of the hot chamber. Thus, the liquid specific work, $W_{air}[i]$, smaller than the expansion work due to losses and consumption in the cold chamber due to the return of the piston, proportionally increases to the expansion work. Considering helium as working fluid, under the same air turn round conditions, Fig. 11 was obtained. In this figure, a similar behavior to air is shown, but with a higher availability of work of the cycle. Comparing Fig. 10 and 11, it can be observed that the specific expansion work produced by helium is about 7 times bigger than that produced by air considering equal masses of the substances contained in the engine. In the experimental part it was observed the highest rotation of the studied motor operating with the helium.

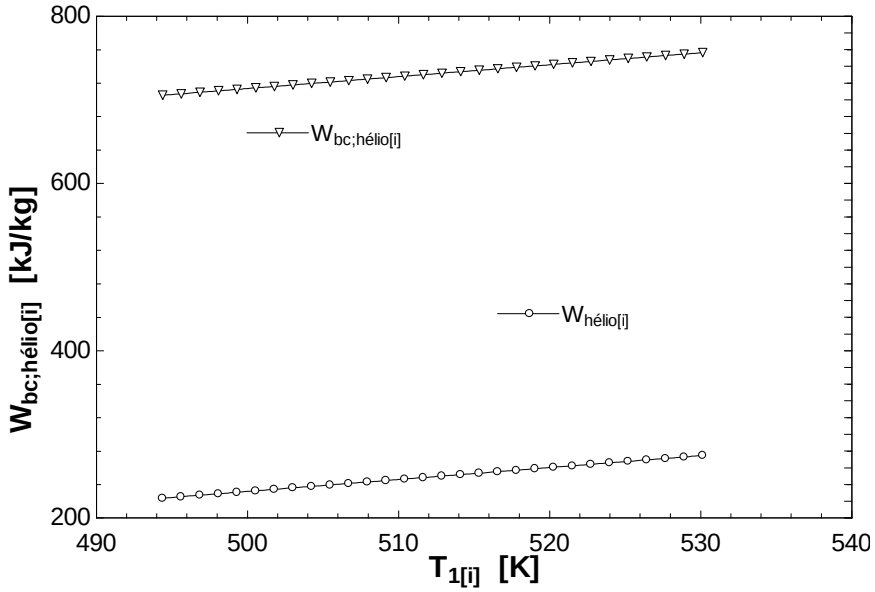

Figure 11 – Graphic showing specific work produced in the expansion $Wbc_{Helium}[i]$ and specific work made available by the engine, $W_{Helium}[i]$, after use this work in the cold chamber (cylinder-piston return assembly) for the engine working with Helium.

Figure 12 shows the efficiency of the alpha type Stirling engine studied as a function of the temperature measured in the hot chamber. The increase in engine efficiency with increasing temperature is observed. This behavior is observed because the thermodynamic model was developed considering that the expansion and compression processes are reversible and adiabatic. Condition not observed on actual motor. In addition, the temperature of the constant cold chamber also influences the observed behavior. The actual engine has presented lower efficiency than calculated.

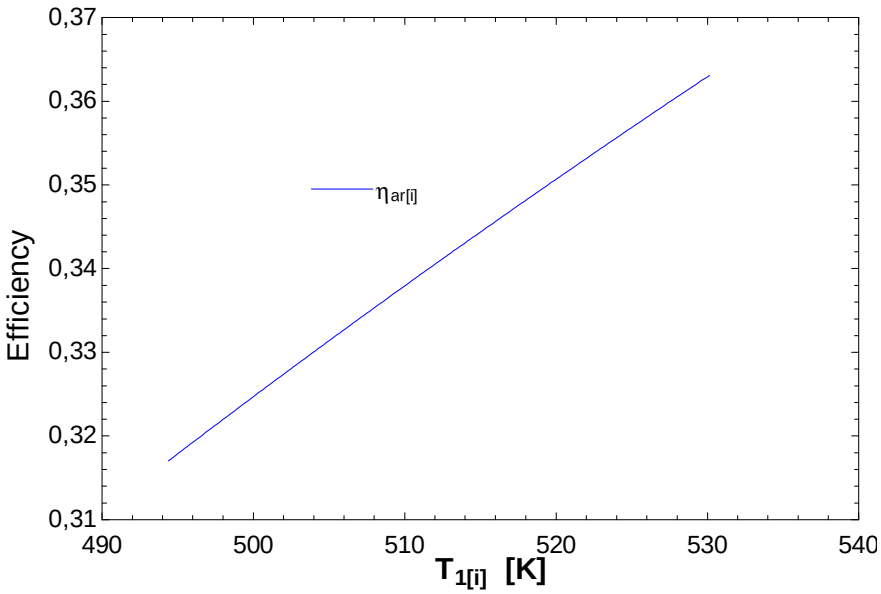

Figure 12 – Graphic showing Engine output calculated through the thermodynamic model developed for air as work fluid.

The results presented in Fig. 10, 11 and 12 have shown the variations of the main parameters studied as a function of the hot chamber temperature. However, due to the difficulty of simultaneous measurements of parameters associated to the engine and internal temperatures to the device, the present study was limited only to a comparative analysis between the fluids used from the data analysis obtained by the motor simulation model and these experimental ones obtained.

5. CONCLUSIONS

The results obtained in the analytical computational simulation and the experimental results have presented deviations in the order of 17.4% for the same turn round conditions considering air as working fluid. This divergence is

consistent due to the losses associated with irreversibility in the actual engine. However, with optimization, it can be observed that under specific conditions (difficult to reach from practice), the cycle can reach high yields mainly by reducing the differences in temperature between the sources. However, working with sources at low temperature, the work generated is reduced and difficult to use in practice.

6. REFERENCES

Ahmadi M. H. *et al. Connectionist intelligent model estimates output power and torque of Stirling engine.* Renewable and Sustainable Energy Reviews Volume 50, October 2015, Pages 871-883.
Ahmadi M. H. *et al. Designing a solar powered Stirling heat engine based on multiple criteria: Maximized thermal efficiency and power.* Energy Conversion and Management. Volume 75, November 2013, Pages 282-291
Duarte L. G. B. *et al. Conversão de energia térmica em energia elétrica utilizando motor Stirling.* Universidade Tecnológica Federal do Paraná (UTFPR). 2013.
Duffie J. A. and Beckman W. A. *Solar engineering of thermal processes.* 2ª Edição, Editora Jonh Wiley & Sons, Inc., New York, Estados Unidos da América, 1991.
Erbay L. B. and Yavuz H. *Analysis of the Stirling heat engine at maximum power conditions.* Energy Volume 22, Issue 7, July 1997, Pages 645-650.
Garg H. P. *Advances in solar energy technology - Vol. 2 Industrial applications of solar energy*. Ed. D. Reidel Publishing Company, Dordrecht, Holanda, 1987.
Holland, J. H. *Adaptation in Natural and Artificial Systems*. Ann Arbor: *University of Michigan Press*, 1975.
Kongtragool B. and Wongwises S. *Thermodynamic analysis of a Stirling engine including dead volumes of hot space, cold space and regenerator.* Renewable Energy Volume 31, Issue 3, March 2006, Pages 345-359.
Parlak N. *et al. Thermodynamic analysis of a gamma type Stirling engine in non-ideal adiabatic conditions.* Renewable Energy Volume 34, Issue 1, January 2009, Pages 266-273.
Soontag, R. E., Borgnakke, C. *Introdução à Termodinâmica para Engenharia.* LTC Editora. Rio de Janeiro, Brasil, 2003.
Tlili I. *et al. Analysis and design consideration of mean temperature differential Stirling engine for solar application.* Renewable Energy Volume 33, Issue 8, August 2008, Pages 1911-1921.

7. RESPONSIBILITY NOTICE

The authors are the only responsible for the printed material included in this paper.